

Measurement of Surface Photovoltage by Atomic Force Microscopy under Pulsed Illumination

Zeno Schumacher,* Yoichi Miyahara, Andreas Spielhofer, and Peter Grutter

McGill University, Montreal H3A 2T8, Canada

(Received 13 January 2016; revised manuscript received 24 February 2016; published 28 April 2016)

Measuring the structure-function relation in photovoltaic materials has been a major drive for atomic force microscopy (AFM) and Kelvin-probe force microscopy (KPFM). The local surface photovoltage (SPV) is measured as the change in contact potential difference (CPD) between the tip and sample upon illumination. The quantities of interest that one will like to correlate with the structure are the decay times of SPV and/or its wavelength dependence. KPFM depends on the tip and sample potential; therefore, SPV is prone to tip changes, rendering an accurate measurement of SPV challenging. We present a measurement technique which allows us to directly measure the difference in the CPD between illuminated and dark states and, thus, SPV as well as the capacitance derivative by using pulsed illumination. The variation of the measured SPV can be minimized due to the time-domain measurement, allowing accurate measurements of the SPV. The increased accuracy enables the systematic comparison of SPV across different measurement setups and excitation conditions (e.g., wavelength dependence and decay time of SPV).

DOI: [10.1103/PhysRevApplied.5.044018](https://doi.org/10.1103/PhysRevApplied.5.044018)

I. INTRODUCTION

The structure-function relationship of photoactive materials is of great interest and can be studied with atomic force microscopy (AFM) [1–6]. Two main modes of measurement can be used: photocurrent and photovoltage measurements. Photoconductive atomic force microscopy (PC AFM) was first presented by Sakaguchi *et al.* [7] in 1999 using a conductive AFM to measure the photocurrent of organic thin films. Photoconductive AFM was later used by Coffey *et al.* [8] to map the photocurrent distribution in an organic photovoltaic blend with approximately 20-nm resolution. In 2013, Beinik *et al.* [9] used PC AFM to investigate the response of ZnO nanorods in a time range greater than seconds.

In contrast to photoconductive AFM, photovoltage measurements can be performed without contact between the sample and the AFM tip. Kelvin-probe force microscopy (KPFM) has become a widely used technique to study not only inorganic but also organic photovoltaic materials [1,3,5,10]. In particular, surface photovoltage (SPV) measurement is commonly used to measure minority-carrier diffusion length [11] and lifetime under illumination in semiconductors [12–14]. The spatially resolved measurement of carrier lifetime and local recombination rates are of great interest to understand the fundamental charge generation process in photovoltaic materials. SPV values are the result of two measurements typically performed consecutively: $SPV = CPD_{\text{illuminated}} - CPD_{\text{dark}}$ where CPD is the contact potential difference between the AFM tip and sample. The CPD is measured using KPFM in which a

dc-bias voltage (KPFM signal) minimizing the electrostatic force is determined with a feedback circuit.

Note that the CPD is the difference between the tip potential and the sample potential—an intrinsic assumption of CPD measurements using KPFM is, thus, that the tip potential remains constant. This assumption is often violated due to the time it takes to measure the spatial dependence of SPV, its wavelength dependence, or decay times. Note that even under an ultra-high-vacuum condition, tip contamination by adsorption of rest gas atoms can change the tip potential (i.e., the work function) in less than a minute [15]. The accuracy of a SPV measurement is, thus, ultimately limited by the stability of the tip surface potential during the time it takes to measure $CPD_{\text{illuminated}}$ and CPD_{dark} . Measurement times can extend over multiple hours or days when the SPV is investigated under various illumination conditions, such as light intensity, wavelength, or polarization, or changes in the sample environment such as the temperature or electric field. Therefore, a measurement method which is insensitive to such tip surface potential changes is needed.

Takahara *et al.* [16] presented a method to measure the local carrier lifetime with SPV and AFM by using pulsed illumination. By varying the repetition rate of the pulse illumination and measuring the average KPFM signal, a higher time resolution than the KPFM feedback time constant can be achieved. This method has also been used on silicon nanocrystal solar cells [17] and organic photovoltaic materials to study local carrier-recombination rates [10]. Note that the accuracy of the SPV measurement determines the temporal resolution achievable with this approach.

A further limiting factor of conventional SPV measurements based on KPFM is that they are only sensitive to a

*zenos@physics.mcgill.ca

change in CPD. However, photocarriers can also contribute to a change in tip-sample capacitance [1]. This change in the capacitance gradient can be measured only if KPFM is performed in bias spectroscopy mode or if the second harmonic signal is measured, which is proportional to the capacitance gradient [18]. As we will show below, a change in the capacitance gradient can lead to a potential systematic error in SPV measurements using established KPFM techniques.

In the following, we present a time-domain KPFM (TD KPFM) approach allowing accurate measurement of the SPV by eliminating the need of a separate reference CPD measurement under dark conditions. TD KPFM takes advantage of pulsed illumination and allows the simultaneous acquisition of full Kelvin-probe force spectra at the same spot under dark and illuminated conditions eliminating the effect of the varying tip potential and capacitance. The change in CPD and capacitance under illumination is measured with TD KPFM.

II. KPFM WITH PULSED ILLUMINATION

KPFM measures the CPD by minimizing the electrostatic interaction between the AFM tip and sample. This is achieved by applying an ac voltage between the tip and sample and minimizing the resulting modulated electrostatic force (F_ω) with a dc bias controlled by a feedback circuit. The applied dc bias yielding a minimum F_ω is equal to the CPD and is independent of the capacitance,

$$F_\omega = \frac{dC}{dz} (V_{dc} - V_{CPD}) V_{ac} \sin(\omega t). \quad (1)$$

Under illumination, a change in the capacitance gradient as well as a change in the CPD are expected [1,3]. Applying a pulsed illumination with the period of T modulates F_ω between two values and can be written as

$$F_\omega = \begin{cases} \frac{dC}{dz} (V_{dc} - V_{CPD}) V_{ac} \sin(\omega t), & \text{light off,} \\ \frac{dC^*}{dz} (V_{dc} - V_{CPD}^*) V_{ac} \sin(\omega t), & \text{light on,} \end{cases} \quad (2)$$

with V_{CPD}^* and dC^*/dz indicating the CPD and capacitance gradient under illumination. Here we assume that the on:off ratio ($T/2$) is unity. As F_ω is measured by a lock-in amplifier, the response time of the feedback τ_{KPFM} is limited by the response time of the lock-in amplifier τ_{loc} .

Since the CPD is now also modulated, we can distinguish between the two cases. When $\tau_{loc} \ll T/2$, the lock-in amplifier can follow the change in CPD, resulting in two distinct values of the KPFM signal that correspond to V_{CPD} and V_{CPD}^* . This condition will, however, limit the pulse rate of the light illumination since the time constant for KPFM feedback is usually fairly slow (greater than a millisecond).

For the case when $\tau_{loc} \gg T/2$, the lock-in amplifier will not be able to react to the change in amplitude in F_ω .

Hence, it will not resolve two distinct values of V_{CPD} and V_{CPD}^* but rather the average of these two values. One might assume this should be the mean of the two CPD values, since the KPFM output is not influenced by the capacitance gradient. However, the output of the lock-in amplifier is a time-averaged value, which can be described by an integration over a full period yielding an averaged F_ω of

$$\langle F_\omega \rangle = \frac{1}{2} \frac{dC}{dz} (V_{dc} - V_{CPD}) V_{ac} + \frac{1}{2} \frac{dC^*}{dz} (V_{dc} - V_{CPD}^*) V_{ac}. \quad (3)$$

The KPFM feedback loop will now try to minimize $\langle F_\omega \rangle$ from Eq. (3). It becomes clear that not only the two CPD values but also the capacitance gradient contributes to the average measured value. A change in dC/dz will change the contribution of the two CPD values to the averaged measurement. The minimum of $\langle F_\omega \rangle$ appears at

$$V_{dc} = \frac{dC/dz V_{CPD} + dC^*/dz V_{CPD}^*}{dC/dz + dC^*/dz}. \quad (4)$$

Therefore, V_{dc} of the KPFM output under pulsed illumination is not only sensitive to the change in CPD but also to a change in the capacitance gradient. Hence, the surface photovoltage under pulsed illumination does not solely reflect the change in CPD and can lead to an inaccurate interpretation. Only when there is no change in the capacitance gradient, the KPFM signal will be the average of the two CPD values, $V_{dc} = (V_{CPD} + V_{CPD}^*)/2$.

In the following, we present a method based on time-domain spectroscopy that avoids these issues and enables a rapid and accurate measurement of SPV.

III. MODULATION OF ELECTROSTATIC FORCE DUE TO PULSED ILLUMINATION

In contrast to KPFM, which solely measures the CPD, frequency-shift bias spectroscopy (also called Kelvin-probe force spectroscopy, KPFS) can be performed to gain information about the CPD and the second derivative of the capacitance. The frequency shift caused by electrostatic force Δf_e is measured as a function of the applied tip-sample dc bias, resulting in a full Kelvin parabola according to [19]

$$\Delta f_e \propto \frac{dF}{dz} = -\frac{1}{2} \frac{d^2C}{dz^2} (V_{dc} - V_{CPD})^2. \quad (5)$$

Fitting Eq. (5) to the experimental data results in the CPD V_{CPD} and the second derivative of the capacitance, d^2C/dz^2 . Recall that both the CPD and capacitance gradient change under illumination.

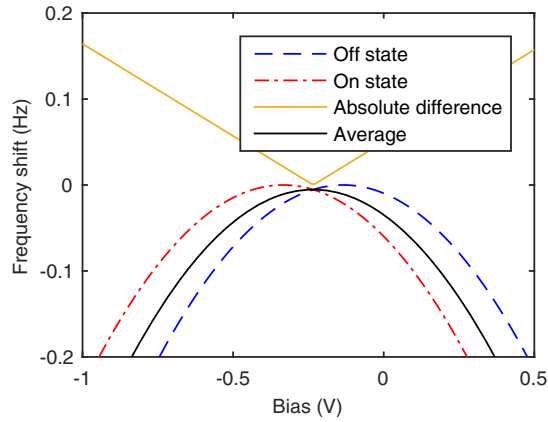


FIG. 1. Simulated frequency-shift bias spectroscopy for a CDP shift of 200 mV. For illustration purposes, the capacitance gradient is kept constant. A pulsed illumination will modulate the frequency shift at any dc bias between the two curves.

This shift in CPD is illustrated with two KPFS curves in Fig. 1. For simplification, only a shift in CPD (and not the effect of the capacitance gradient) is considered here. As one can see from Fig. 1, for each value of the applied bias a different frequency shift is expected for the two states. A pulsed illumination under a constant dc bias will, therefore, modulate the frequency shift at the rate of the pulsed illumination between the two curves. The modulation frequency can be freely chosen so that the modulation is faster than the time interval between the tip changes but long enough to reach the steady-state value. This modulation effectively implements a sort of common-mode rejection measurement, eliminating tip (or sample) CPD changes with a longer time constant than the modulation time scale. The detection bandwidth of the frequency detector needs to be higher than the modulation frequency to ensure the measured Δf is following the modulation. The strength of the modulation is equal to the difference in the CPD between the two states. The electrostatically induced frequency shift can be written similarly to Eq. (2) without the V_{ac} modulation,

$$\Delta f_e \propto \begin{cases} \frac{d^2C}{dz^2} (V_{dc} - V_{CPD})^2, & 0 < t < T/2, \\ \frac{d^2C^*}{dz^2} (V_{dc} - V_{CPD}^*)^2, & T/2 < t < T. \end{cases} \quad (6)$$

The modulation between the two states (Δf_{on} and Δf_{off}) can be measured in the frequency or time domain as described below.

A. Frequency domain measurement

Since the modulation is driven by a square wave (pulsed illumination), Δf is modulated at the frequency of the light illumination (ν) and every odd harmonic. The fundamental harmonic component can be described as

$$\Delta f_\nu = \frac{4}{\pi} (\Delta f_{off} - \Delta f_{on}) \sin(\nu t), \quad (7)$$

and can be detected by a lock-in amplifier. It becomes clear that the strength of the modulation at Δf_ν is proportional to the difference in the frequency shift between the two states. A frequency domain measurement can be used to measure the absolute value of the difference (see Fig. 1) between the two states when sweeping the bias (e.g., between the two curves). Such a frequency domain measurement will reject any unwanted tip or sample changes if the modulation frequency is chosen high enough. However, the measurement is still a convolution of the change in the CPD and capacitance gradient.

B. Time domain KPFS

The desired signal, the Δf value for both Kelvin parabola, can be recovered from the Δf channel in the time domain. Instead of measuring the time-averaged signal of the CPD by KPFS, Δf can be integrated over a short time interval after it reaches each steady state, V_{CPD} and V_{CPD}^* in the dark and illuminated state, respectively, as shown in Eq. (8). The integration over a short time in each state yields the two curves corresponding to V_{CPD} and V_{CPD}^* . The integration needs to be performed after the Δf values reach their steady state so that the results are not influenced by the transient values or the delay between the pulses,

$$\begin{aligned} \Delta f_{on} &\propto \frac{1}{b-a} \int_a^b -\frac{1}{2} \frac{d^2C}{dz^2} (V_{dc} - V_{CPD})^2 dt, \\ \Delta f_{off} &\propto \frac{1}{b-a} \int_{a+t/2}^{b+t/2} -\frac{1}{2} \frac{d^2C^*}{dz^2} (V_{dc} - V_{CPD}^*)^2 dt. \end{aligned} \quad (8)$$

Such an integration of Δf over a short time interval at a defined time within a modulation period can experimentally be realized by a gated integration (see Fig. 2). Within a reference period, the start and duration of the integration can be defined in terms of phase. Here the modulation signal for the pulsed illumination acts as the reference signal. Generally, any modulation (electrical, illumination, thermal, etc.) can be used as a reference signal.

One gated integration interval is set within the illumination-on state, whereas the second integration interval is set within the illumination-off state. This coincides with Δf reaching a maximum or minimum, respectively. A third integrator is set longer than a modulation period to obtain the averaged curve, if desired. The output of each integrator is recorded before the applied bias is changed.

Similar to a regular KPFS measurement, Δf can be integrated at each applied V_{dc} to reconstruct the full Kelvin parabola. In particular, with two different integrations, two curves are acquired, one for V_{CPD} and one for V_{CPD}^* . A

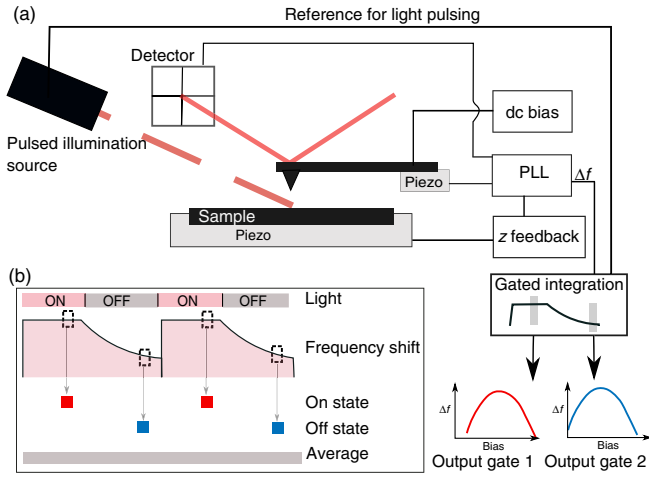


FIG. 2. (a) Block diagram of the TD KPFM measurement. The frequency-shift signal is integrated with two gated integrations synchronized with the pulsed illumination. Each output of the gated integration is recorded at each applied bias to record a full Kelvin parabola. (b) Measurement scheme for a gated integration in the time domain of the modulated frequency shift.

schematic of the TD KPFM measurement is shown in Fig. 2.

IV. RESULTS AND DISCUSSION

As CPD is a relative measurement between a tip and sample, it is possible to measure a photoactive tip. A nonphotoactive sample (cleaved KBr) and a photoactive tip (silicon cantilever) are used to demonstrate an implementation of TD KPFM. The photo absorption in silicon cantilevers under ultra-high-vacuum on a JEOL JSPM-4500A is measured. SPV measurements of silicon were previously reported with metal coated cantilevers [6]. The tip-sample junction is illuminated with a laser at 580 nm, 2.5 mW (FemtoFiber pro TVIS, Toptica), modulated by an optical chopper at 500 Hz. A 50/50 duty cycle is used, resulting in an illumination duration of 1 ms followed by a 1-ms long dark state. The chopper rate is chosen to guarantee the Δf signal reaches its steady state and is not influenced by the time between the pulses. A fast digital lock-in amplifier (UHF, Zurich Instruments) is used as the phase-locked loop (PLL) with a bandwidth of 1 kHz to measure the cantilever frequency. The PLL bandwidth must be set higher than the modulation frequency. The boxcar integration option (UHF-BOX Boxcar Averager, Zurich Instruments) with two gated integrators is used to implement the measurements of Δf_{on} and Δf_{off} [see Eq. (8)]. The starting phase of each of the two integrators is set so that the signal is integrated around the maximum or minimum of the frequency shift. The output of the two boxcar units is recorded with a Nanonis scan controller. When sweeping the bias, three frequency shift vs bias curves are recorded simultaneously: the two gated

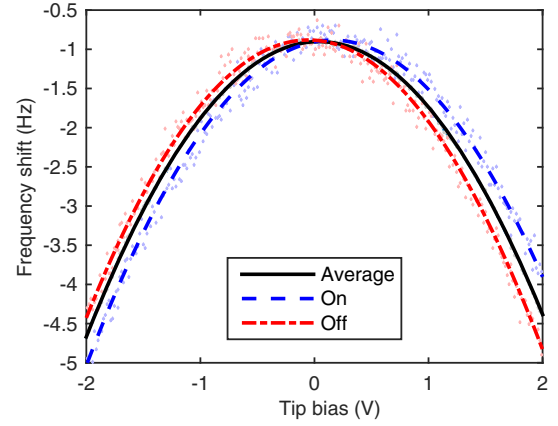


FIG. 3. TD KPFM measurement of the SPV under pulsed illumination. A gated integration is used to acquire the bias spectroscopy for the dark and illuminated states simultaneously. A shift of 213 ± 4 mV in the CPD and 5% in $(d^2C)/(dz^2)$ is measured under illumination.

integrations containing information about the two different states and the average of the frequency-shift signal. Figure 3 shows the measured data and a fitted parabola for each data set. A shift of 213 ± 4 mV in CPD and 5% change in $(d^2C)/(dz^2)$ is measured under illumination. This change in $(d^2C)/(dz^2)$ is not detected in the SPV measurement using standard KPFM.

To illustrate the robustness of TD KPFM, bias spectroscopy measurements are performed for more than 18 consecutive hours. Figure 4 shows a histogram of a simultaneously acquired SPV measurement by TD KPFM and a standard SPV measurement with just one reference measurement at the beginning, repeated 162 times over more than 18 hours. The inset shows two measurements at

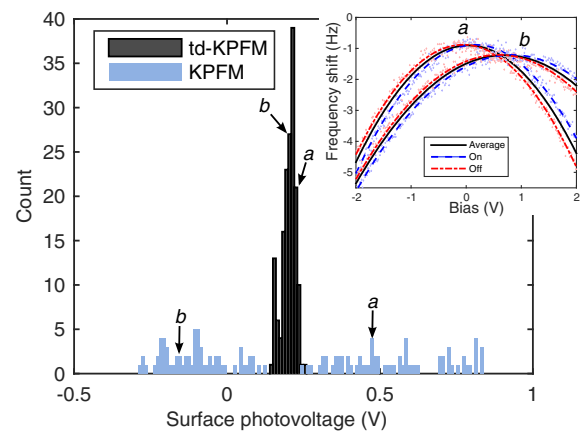


FIG. 4. Histogram of 162 SPV measurements recorded successively over more than 18 h. The differential TD KPFM SPV measurement (202 ± 22 mV) has a much higher precision than the standard SPV measurement (207 ± 312 mV) with a 14-times-smaller standard deviation. The inset shows two measurements *a* and *b* at different times.

different times indicated by a and b in the histogram. The average CPD is significantly different between the measurements; however, the difference measured between the on and off state by TD KPFM is not. No spatial drift correction is used during this measurement to test the TD KPDM under the most unfavorable condition. The standard SPV measurement shows a large spread due to a large variability of CPD over time (due to drift and tip or sample contact potential changes), whereas the differential TD KPFM measurement is showing a very narrow distribution with a 14-times-smaller standard deviation. The spread in the TD KPFM SPV data originates from a fluctuation of the illumination intensity [13], whereas the KPFM SPV data are also affected by any unwanted slowly varying tip or sample changes. The decreased standard deviation over such a long measurement time is indispensable for studies of changes in the SPV under different illumination conditions (wavelength, intensity, etc.) or sample environment.

V. CONCLUSION

We present a time-domain measurement of a SPV by AFM using a simple-to-implement gated integration method (TD KPFM). This differential TD KPFM measurement of the SPV increases the accuracy by more than an order of magnitude, as it is independent of drift in the tip or sample work function, since it measures only the change in the CPD under modulated illumination. As a demonstration of TD KPFM, we measure the SPV of naturally oxidized silicon over many hours in UHV. Regular KPFM determines a SPV of 207 ± 312 mV, whereas our differential TD KPFM method obtains 202 ± 22 mV, an order of magnitude improvement in accuracy. Achieving this accuracy opens the possibility to compare SPV measurements of the same sample with different tips and even across different laboratories, a crucial step if quantitative theoretical modeling and, thus, physical interpretation of SPV results is to be achieved.

Our analysis of the KPFM theory under pulsed illumination suggests that the output of KPFM is no longer independent of the tip-sample capacitance. Capacitance changes are the result of photon-generated charges in the sample or tip. The technique introduced here, TD KPFM, allows the measurement of true CPD changes under pulsed illumination without the systematic error inherent in standard KPFM due to tip-sample capacitive changes. It is important to note that any measured CPD by KPFM under pulsed illumination is affected by the change in capacitance in any sample and is not limited to inorganic semiconductors. Hence, it is crucial to quantify the change in capacitance to get the true change in the CPD if pulsed illumination is used. Recently presented minority-carrier lifetime measurements [10,16,17] all rely on pulsed illumination. Thus, TD KPFM should be used for such minority-carrier lifetime measurements. By making SPV

measurements independent of tip effects, TD KPFM will greatly improve the accuracy and time resolution of carrier lifetime measurement.

We note that this time-domain approach of measuring a modulation in AFM is not limited to SPV and KPFM measurements. It can be extended to any modulation of the tip-sample interaction, such as electric or thermal pulses. Especially for cases with square wave modulation, where lock-in techniques measure only the first Fourier component, this gated time-domain approach can be of great interest. With this gated time-domain approach, the absolute values of the modulated signal (e.g., frequency shift, CPD, etc.) can be recovered rather than just the strength of the modulation (e.g., average CPD, etc.). This is demonstrated with TD KPFM where the CPD and $(d^2C)/(dz^2)$ values are recorded instead of the average CPD over the modulation. When such pulses are used to study decay times, the increased accuracy will allow a better determination of the time-dependence reaction of the system to these pulses, e.g., mobility if the potential is pulsed or minority-carrier lifetime if the illumination is pulsed.

ACKNOWLEDGMENTS

The authors thank the NSERC and FQRNT for funding. Z. S. thanks the Swiss National Science Foundation for a DOC.Mobility Fellowship.

-
- [1] David C. Coffey and David S. Ginger, Time-resolved electrostatic force microscopy of polymer solar cells, *Nat. Mater.* **5**, 735 (2006).
 - [2] V. Palermo, M. Palma, and P. Samorì, Electronic characterization of organic thin films by Kelvin probe force microscopy, *Adv. Mater.* **18**, 145 (2006).
 - [3] Sarah A. Burke, Jeffrey M. LeDue, Jessica M. Topple, Shawn Fostner, and Peter Grütter, Relating the functional properties of an organic semiconductor to molecular structure by nc-AFM, *Adv. Mater.* **21**, 2029 (2009).
 - [4] Satoshi Watanabe, Yasumasa Fukuchi, Masako Fukasawa, Takafumi Sassa, Atsushi Kimoto, Yusuke Tajima, Masanobu Uchiyama, Takashi Yamashita, Mutsuyoshi Matsu-moto, and Tetsuya Aoyama, *In situ* KPFM imaging of local photovoltaic characteristics of structured organic photovoltaic devices, *ACS Appl. Mater. Interfaces* **6**, 1481 (2014).
 - [5] Alex Henning, Gino Günzburger, Res Jöhr, Yossi Rosenwaks, Biljana Bozic-Weber, Catherine E. Housecroft, Edwin C. Constable, Ernst Meyer, and Thilo Glatzel, Kelvin probe force microscopy of nanocrystalline TiO₂ photoelectrodes, *Beilstein J. Nanotechnol.* **4**, 418 (2013).
 - [6] Christian Loppacher, Ulrich Zerweck, Sebastian Teich, Elke Beyreuther, Tobias Otto, Stefan Grafström, and Lukas M. Eng, FM demodulated Kelvin probe force microscopy for surface photovoltage tracking, *Nanotechnology* **16**, S1 (2005).

- [7] Hiroshi Sakaguchi, Futoshi Iwata, Atsushi Hirai, Akira Sasaki, and Toshihiko Nagamura, Nanometer-scale photoelectric property of organic thin films investigated by a photoconductive atomic force microscope, *Jpn. J. Appl. Phys.* **38**, 3908 (1999).
- [8] David C. Coffey, Obadiah G. Reid, Deanna B. Rodovsky, Glenn P. Bartholomew, and David S. Ginger, Mapping local photocurrents in polymer/fullerene solar cells with photoconductive atomic force microscopy, *Nano Lett.* **7**, 738 (2007).
- [9] Igor Beinik, Markus Kratzer, Astrid Wachauer, Lin Wang, Yuri P. Piryatinski, Gerhard Brauer, Xin Yi Chen, Yuk Fan Hsu, Aleksandra B. Djurišić, and Christian Teichert, Photoresponse from single upright-standing ZnO nanorods explored by photoconductive AFM, *Beilstein J. Nanotechnol.* **4**, 208 (2013).
- [10] Guozheng Shao, Micah S. Glaz, Fei Ma, Huanxin Ju, and David S. Ginger, Intensity-modulated scanning Kelvin probe microscopy for probing recombination in organic photovoltaics, *ACS Nano* **8**, 10799 (2014).
- [11] Alvin M. Goodman, A method for the measurement of short minority carrier diffusion lengths in semiconductors, *J. Appl. Phys.* **32**, 2550 (1961).
- [12] E. O. Johnson, Measurement of minority carrier lifetimes with the surface photovoltage, *J. Appl. Phys.* **28**, 1349 (1957).
- [13] Dieter K. Schroder, Surface voltage and surface photovoltage: History, theory and applications, *Meas. Sci. Technol.* **12**, R16 (2001).
- [14] Leor Kronik, Surface photovoltage phenomena: Theory, experiment, and applications, *Surf. Sci. Rep.* **37**, 1 (1999).
- [15] William Paul, Yoichi Miyahara, and Peter Grütter, Implementation of atomically defined field ion microscopy tips in scanning probe microscopy, *Nanotechnology* **23**, 335702 (2012).
- [16] Masaki Takihara, Takuji Takahashi, and Toru Ujihara, Minority carrier lifetime in polycrystalline silicon solar cells studied by photoassisted Kelvin probe force microscopy, *Appl. Phys. Lett.* **93**, 021902 (2008).
- [17] L. Borowik, H. Lepage, N. Chevalier, D. Mariolle, and O. Renault, Measuring the lifetime of silicon nanocrystal solar cell photo-carriers by using Kelvin probe force microscopy and x-ray photoelectron spectroscopy, *Nanotechnology* **25**, 265703 (2014).
- [18] Todd Hochwitz, Alber K. Henning, Chris Levey, Charles Daghlian, James Slinkman, James Never, Phil Kaszuba, Robert Gluck, Randy Wells, Pekarik John, and Robert Finch, Imaging integrated circuit dopant profiles with the force-based scanning Kelvin probe microscope, *J. Vac. Sci. Technol. B* **14**, 440 (1996).
- [19] Shinichi Kitamura and Masashi Iwatsuki, High-resolution imaging of contact potential difference with ultrahigh vacuum noncontact atomic force microscope, *Appl. Phys. Lett.* **72**, 3154 (1998).